INTERNATIONAL JOURNAL FOR NUMERICAL AND ANALYTICAL METHODS IN GEOMECHANICS, VOL. 15, 457–470 (1991)

# RESPONSE OF CIRCULAR FOOTINGS AND ANCHOR PLATES IN NON-HOMOGENEOUS ELASTIC SOILS

R. K. N. D. RAJAPAKSE

*Department of Civil Engineering, University of Manitoba, Winnipeg, R3T 2N2, Canada*

AND

A. P. S. SELVADURAI

*Department of Civil Engineering, Carleton University, Ottawa, KIS 5B6, Canada*

## SUMMARY

The axisymmetric elastic response of circular footings and anchor plates in a linearly non-homogeneous elastic soil is analysed. It is assumed that footings/anchors are flexible and subjected to axisymmetric vertical loads. The response of the footing/anchor is modelled by using the classical Poisson–Kirchhoff thin plate theory. A variational technique is used to analyse the interaction problem. A representation for the contact stress is established by using a fundamental solution corresponding to a unit vertical pressure acting over an annular region in the interior of the non-homogeneous soil. The fundamental solution can be derived by using rigorous analytical procedures. The influence of the footing flexibility and the degree of soil non-homogeneity on the displacements, bending moments and contact stresses of a surface footing is examined over a wide range of governing parameters. In the case of anchor plates the influence of depth of embedment, degree of soil non-homogeneity and anchor flexibility on the anchor displacement is investigated.

## INTRODUCTION

The study of interaction between a circular elastic plate and an elastic medium has useful applications in geotechnical engineering. For example, the plate–elastic medium model can be used to simulate the working load response of surface or embedded foundations, anchor plates resisting uplift loads and theoretical modelling of some *in situ* testing methods. A variety of analytical, semi-analytical and numerical methods can be used to analyse the plate–elastic medium interaction problem. Selvadurai[1] presents a comprehensive review of elastic methods of analysis applicable to the present class of problems. It is noted that nearly all of the existing studies are concerned with plates resting on or embedded within a homogeneous elastic medium.

Experimental investigations by Skempton and Henkel,[2] Ward *et al.*,[3,4] Burland and Lord[5] and Abbiss[6] indicate that the undrained Young's modulus of many naturally occurring soil deposits increases approximately linearly with depth. The importance of the incorporation of soil heterogeneity into geotechnical analysis has been recognized in the past.[7] Gibson[8] presented a fundamental study on the response of a linearly non-homogeneous incompressible elastic soil subjected to a vertical load at the surface level. Subsequent studies[9–14] considered a variety of problems associated with linearly non-homogeneous incompressible and compressible soil media subjected to surface loading. The complexity associated in the derivation of fundamental elastic solutions for buried loading has restricted the development of elastic solutions corresponding to a variety of non-homogeneous soil–structure interaction problems.

0363–9061/91/070457–14$07.00


*Received 22 March 1990*
*Revised 22 August 1990*

A review of the literature indicates that the class of problems related to the interaction between an elastic circular plate and a non-homogeneous elastic medium has not been considered previously. Rowe and Booker[15] analysed the elastic response of single and multiple underreamed rigid anchors in a linearly non-homogeneous elastic soil (Gibson soil). The anchor was modelled as a system of annular regions subjected to uniform vertical pressure. The displacement influence functions required in the analysis were numerically evaluated by treating the non-homogeneous medium as a multilayered elastic medium. Solutions for circular patch loadings and rigid circular footings on a non-homogeneous elastic soil with a crust were also given by Rowe and Booker.[16] In this paper the authors present a unified treatment of the elastic plate–non-homogeneous soil interaction problem. Consideration will be given to circular footings resting on the surface of the soil as well as to anchor plates located at a finite depth below the soil surface as shown in Figure 1. The shear modulus of the isotropic soil medium is assumed to vary linearly with depth and the medium is considered to be incompressible (Poisson's ratio is equal to 0·5). The latter assumption simulates the undrained deformations of saturated soils and other geological media.

The analysis presented in this paper is based on a variational method of analysis developed by Selvadurai[17] for an elastic plate resting on a half-space. The solution scheme[17] has been recently modified by Rajapakse[18] into an efficient matrix formulation to analyse embedded plates as well as plates with edge restraints such as those provided by a basement wall, storage tank walls and a central rigid core. In the analysis the displacement of the plate is represented by an admissible function of the radial co-ordinate containing a set of generalized co-ordinates. The contact pressure corresponding to each term of the assumed displacement function is evaluated by dividing the contact surface into several concentric annular rings with uniform pressure distribution and solving a flexibility equation for the soil medium. The influence function required to establish the flexibility equation corresponds to the vertical displacement due to unit vertical pressure acting over an annular region in the interior of the non-homogeneous soil. An analytical solution for the influence function is presented. The total potential energy function of the plate–elastic soil system is derived by using the assumed displacement function and the representation for contact pressure. The stationary conditions of the energy functional result in a system of linear simultaneous equations which is solved numerically.

Comparisons are presented with solutions given by Rowe and Booker[15] for a rigid circular anchor plate. Thereafter an extensive parametric study is conducted to examine the elastic

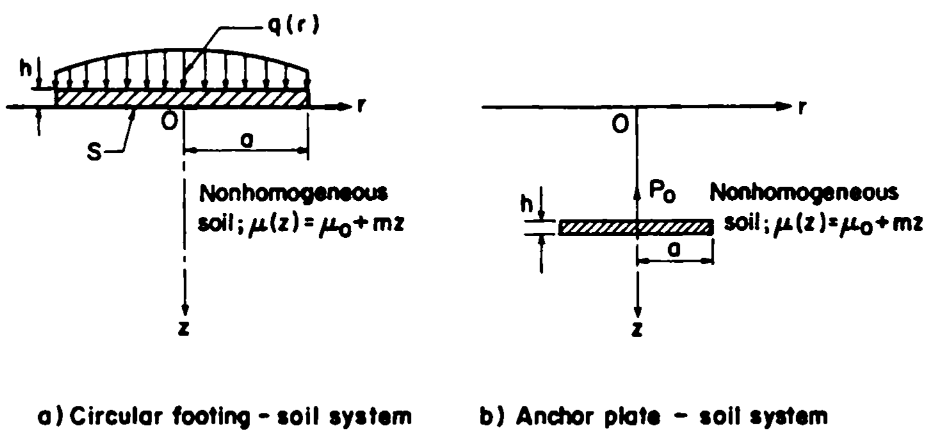


Figure 1. Geometry of the interaction problem

response of the plate–non-homogeneous soil system. Numerical solutions for uniformly loaded and centrally loaded circular footings on the surface of a non-homogeneous soil are presented. The influence of the footing flexibility and the degree of soil non-homogeneity on the footing displacement, bending moments and contact pressure is discussed. For anchor plates the influence of the depth of embedment, degree of soil non-homogeneity and plate flexibility on the anchor displacement is investigated.

## ANALYSIS OF INTERACTION PROBLEM

The plate–non-homogeneous soil interaction problems considered in this paper are shown in Figure 1. The radius of the plate, denoted by $a$, is considered as the unit length parameter. The entire problem including the co-ordinate frame $(r, \theta, z)$ is normalized with respect to $a$. The variational solution procedure used in this paper follows the developments presented previously[17,18] for a homogeneous soil medium. In this section basic steps and relevant equations are outlined. The energy functional is derived on the basis of the kinematically admissible plate deflected shape $w(r)$ given by

$$w(r) = a_0 r^2 \log r + \sum_{n=0}^{N} \alpha_n r^{2n} \tag{1}$$

where $a_0 = P_0/8\pi D$ and $D = E_p h^3/12(1 - \nu_p^2)$.

In equations (1), $\alpha_n$ ($n = 0, 1, 2, \ldots, N$) denotes a set of generalized co-ordinates, $P_0$ is the central vertical force acting on the plate, $h$ is the thickness of the plate and $E_p$ and $\nu_p$ are Young's modulus and Poisson's ratio of the plate material respectively. It may be noted that the representation given by equation (1) incorporates the deflection corresponding to a plate of infinite extent which is subjected to a concentrated force (see e.g. Reference 19). The flexural moments exhibit singular behaviour as $r \to 0$. In the case of plates subjected to distributed loading only (i.e. $P_0 = 0$), the first term of equation (1) vanishes.

It is assumed that the shear modulus $\mu(z)$ of the soil varies linearly with the depth in the following manner:

$$\mu(z) = \mu_0 + mz, \quad m > 0 \tag{2}$$

It can be shown[18] that the strain energy of a thin elastic plate undergoing deformation specified by equation (1) can be expressed as

$$U_p = 21a_0^2/4 + \langle Q^p \rangle \{\alpha\} + \{\alpha\}^T [K^p] \{\alpha\} \tag{3}$$

where

$$\{\alpha\} = \langle \alpha_0 \ \alpha_1 \ \alpha_2 \ \ldots \ \alpha_N \rangle^T \tag{4}$$

and the elements of the row vector $\langle Q^p \rangle$ and the matrix $[K^p]$ are given elsewhere.[18]

The boundary conditions related to the plate edges can be expressed as

$$[B]\{\alpha\} = \{R\} \tag{5}$$

The elements of $[B]$ and $\{R\}$ corresponding to a free edge or some other boundary conditions can be obtained by using equation (1) together with classical thin plate theory.[19]

The contact stress $T_z(r)$ acting on the plate–soil contact surface $S$ can be expressed in terms of generalized co-ordinates $\alpha_n$ as

$$T_z(r) = \sum_{n=0}^{N} \alpha_n T_{nz}(r) + a_0 T^*(r) \tag{6}$$

where $T_{nz}(r)$ and $T^*(r)$ denote the contact stresses corresponding to plate displacement fields $r^{2n}$ and $r^2 \log r$ respectively.

A solution for contact stresses $T_{nz}(r)$ and $T^*(r)$ can be obtained by discretizing the contact area $S$ into $M$ ring elements. The stress $T_{nzi}$ acting on the $i$th ring element is determined by solving the following flexibility equation:

$$[F]\{T_{nz}\} = \{w_n\}, \quad n = 0, 1, 2, \ldots, N \tag{7}$$

The elements $F_{ij}$, $T_{nzi}$ and $w_{ni}$ of $[F]$, $\{T_{nz}\}$ and $\{w_n\}$ are given by

$$F_{ij} = f_{zz}(r_i, H; r_{j1}, r_{j2}) \tag{8}$$

$$T_{nzi} = T_{nz}(r_i) \tag{9}$$

$$w_{ni} = r_i^{2n} \tag{10}$$

In equation (8), $f_{zz}(r_i, H; r_{j1}, r_{j2})$ denotes the vertical displacement at the point $(r_i, H)$ due to unit vertical pressure acting on the $j$th ring element bounded by radii $r_{j1}$ and $r_{j2}$. A solution for $T_{zi}^*$ corresponding to the $i$th ring element is determined by solving equation (7) with $w_{ni} = r_i^2 \log r_i$.

The strain energy of the soil region can be expressed as[18]

$$U_h = \{\alpha\}^{\mathrm{T}}[K^{\mathrm{h}}]\{\alpha\} + \langle Q^{\mathrm{h}}\rangle\{\alpha\} + \pi a_0^2 \sum_{j=1}^{M} r_j^3 T_{zj}^*(r_{j2} - r_{j1}) \log r_j \tag{11}$$

The elements of $[K^{\mathrm{h}}]$ and $\langle Q^{\mathrm{h}}\rangle$ are explicitly given elsewhere.[18]

A constraint energy functional for the plate–soil system which satisfies the plate edge boundary conditions can be expressed as[20]

$$\bar{U} = U_{\mathrm{p}} + U_{\mathrm{h}} - P_0\alpha_0 - 2\pi q_0 \sum_{n=0}^{N} \alpha_n/(2n+2) + \{\lambda\}^{\mathrm{T}}([B]\{\alpha\} - \{R\}) \tag{12}$$

where $\{\lambda\} = \langle \lambda_1 \ \lambda_2 \rangle^{\mathrm{T}}$ is a vector of Lagrange multipliers and $q_0$ is the intensity of uniform distributed load acting on the plate.

At equilibrium, $\bar{U}$ is stationary and the stationary conditions are given by[20]

$$\partial \bar{U}/\partial \alpha_i = 0, \quad i = 0, 1, 2, \ldots, N \tag{13}$$

$$\partial \bar{U}/\partial \lambda_i = 0, \quad i = 1, 2 \tag{14}$$

Substitution of equation (12) in equations (13) and (14) results in

$$\begin{bmatrix} [\bar{K}] & [B]^{\mathrm{T}} \\ [B] & [0] \end{bmatrix} \begin{Bmatrix} \{\alpha\} \\ \{\lambda\} \end{Bmatrix} = \begin{Bmatrix} \{X\} \\ \{R\} \end{Bmatrix} \tag{15}$$

where

$$[\bar{K}] = [K^{\mathrm{p}}] + [K^{\mathrm{p}}]^{\mathrm{T}} + [K^{\mathrm{h}}] + [K^{\mathrm{h}}]^{\mathrm{T}} \tag{16}$$

$$\{X\} = \{P_0 \delta_{1i}\} + \{\pi q_0/i\} - \langle Q^{\mathrm{p}}\rangle^{\mathrm{T}} - \langle Q^{\mathrm{h}}\rangle^{\mathrm{T}} \tag{17}$$

with $\delta_{ij}$ Kronecker's delta function.

Numerical solution of equation (15) yields $\{\alpha\}$ and $\{\lambda\}$ corresponding to a specified geometry and material configuration of the interaction system. The plate displacement, stress resultants and contact pressure can be computed thereafter.

Note that in the above formulation the plate edge boundary conditions are satisfied exactly. This is in contrast to the penalty function formulation presented previously[18] where the penalty number controls the degree of accuracy to which the boundary conditions are satisfied.

## DISPLACEMENT INFLUENCE FUNCTION

The analysis scheme presented above is based on the displacement influence function $f_{zz}(r, H; s_1, s_2)$ corresponding to a unit vertical pressure acting over an annular region in the interior of a linearly non-homogeneous elastic half-space. Consider an annular region $\Omega$ in the non-homogeneous half-space at a depth $z = H$ and bounded by radii $r = s_1$ and $s_2$ ($s_2 > s_1$). A solution for the influence function can be derived by using procedures described elsewhere[21] together with the general solutions[22] for a non-homogeneous medium.

It can be shown that the displacement in the $z$-direction at the point $(r, H)$, denoted by $f_{zz}(r, H; s_1, s_2)$, due to unit vertical pressure acting on the region $\Omega$ is given by

$$f_{zz}(r, H; s_1, s_2) = \int_0^\infty [(-k_1 k_9 + k_2 + \alpha_3) + (k_4 - k_3 k_9 - k_4 k_9) e^{-2\xi(q_1 - q_0)}] C_1 J_0(\xi r) d\xi \quad (18)$$

where

$$C_1 = \frac{\xi[s_1 J_1(\xi s_1) - s_2 J_1(\xi s_2)](\beta_{51} k_5 - \xi k_1 - \xi k_1 k_7)}{2\mu(H) R(\xi, q_0, q_1)} \quad (19)$$

$$k_1 = (\alpha_{60}\beta_{60} + \xi\beta_{30})/\xi(\alpha_{60} + \alpha_{50}) \quad (20)$$

$$k_2 = (\alpha_{60}\beta_{60} + \xi\beta_{40})/\xi(\alpha_{60} + \alpha_{50}) \quad (21)$$

$$k_3 = (\alpha_{50}\beta_{60} - \xi\beta_{30})/\xi(\alpha_{60} + \alpha_{50}) \quad (22)$$

$$k_4 = (\alpha_{50}\beta_{60} - \xi\beta_{40})/\xi(\alpha_{60} + \alpha_{50}) \quad (23)$$

$$k_5 = 2k_1/(\alpha_{21} - \alpha_{41}) \quad (24)$$

$$k_6 = (2k_2 + \alpha_{11} + \alpha_{31})/(\alpha_{21} - \alpha_{41}) \quad (25)$$

$$k_7 = -(\alpha_{41} + \alpha_{21})/(\alpha_{21} - \alpha_{41}) \quad (26)$$

$$k_8 = -(\alpha_{11}\alpha_{41} + \alpha_{31}\alpha_{21})/(\alpha_{21} - \alpha_{41}) \quad (27)$$

$$k_9 = (k_2\xi - \beta_{61} + \xi k_7 k_2 + \xi k_8 - \beta_{51} k_6)/(\beta_{51} k_5 - \xi k_1 - \xi k_7) \quad (28)$$

$$\alpha_{ij} = \alpha_i(q_j), \quad \beta_{ij} = \beta_i(q_j), \quad i = 1, 2, \ldots, 6, \quad j = 0, 1 \quad (29)$$

$$\alpha_1(q) = -[e^{-2\xi q} Ei(2\xi q) + \log(\xi q)] \quad (30)$$

$$\alpha_2(q) = -[e^{2\xi q} Ei(-2\xi q) + \log(\xi q)] \quad (31)$$

$$\alpha_3(q) = e^{-2\xi q} Ei(2\xi q) - \log(\xi q) \quad (32)$$

$$\alpha_4(q) = e^{2\xi q} Ei(-2\xi q) - \log(\xi q) \quad (33)$$

$$\alpha_5(q) = \xi - q^{-1} \quad (34)$$

$$\alpha_6(q) = \xi + q^{-1} \quad (35)$$

$$\beta_1(q) = q^{-1}[\alpha_3(q) - 1] + \xi\alpha_1(q) \quad (36)$$

$$\beta_2(q) = -q^{-1}[\alpha_4(q) - 1] + \xi\alpha_2(q) \quad (37)$$

$$\beta_3(q) = q^{-1}[\alpha_4(q) - 1] + \xi\alpha_2(q) \quad (38)$$

$$\beta_4(q) = q^{-1}[\alpha_3(q) - 1] - \xi\alpha_1(q) \quad (39)$$

$$\beta_5(q) = -[q^{-1} + \xi\alpha_4(q)] \quad (40)$$

$$\beta_6(q) = q^{-1} - \xi\alpha_3(q) \tag{41}$$

$$q_0 = \mu_0/m, \qquad q_1 = H + \mu_0/m \tag{42}$$

$$\begin{aligned} R(\xi, q_0, q_1) = & -\beta_{61}\alpha_{51}k_1 + \xi\alpha_{51}k_1k_8 - \alpha_{51}\beta_{51}k_1k_6 + \alpha_{61}\beta_{51}k_1k_7k_6 \\ & - \beta_{31}k_2k_5\xi + \beta_{61}\beta_{31}k_5 - \xi\beta_{31}k_7k_2k_5 - \xi\beta_{31}k_5k_8 \\ & + \beta_{31}\beta_{51}k_5k_6 + \xi k_1\beta_{41} + \xi\alpha_{61}k_1k_8 + \xi\beta_{31}k_1k_6 \\ & + \xi\beta_{41}k_1k_7 + \xi\beta_{31}k_1k_6k_7 + \alpha_{51}\beta_{51}k_2k_5 - \beta_{51}\beta_{41}k_5 \\ & - \alpha_{61}\beta_{51}k_2k_5k_7 - \alpha_{61}\beta_{51}k_5k_8 - \beta_{51}\beta_{31}k_5k_6 \end{aligned} \tag{43}$$

In equations (18)–(43), $J_n$, $Ei$ and $\xi$ denote Bessel function[23] of the first kind of order $n$, exponential integral[23] and Hankel transform[24] parameter respectively.

## NUMERICAL RESULTS AND DISCUSSION

A computer code based on the above analysis has been developed to study numerically the response of a plate–non-homogeneous soil system. The following non-dimensional quantities are used in the parametric study:

degree of non-homogeneity of soil, $(\bar{m}) = m/\mu_0$
depth of embedment, $\bar{H} = H/a$
relative rigidity parameter, $K_r = E_p(h/a)^3/\mu_0$
plate displacement, $\bar{w}(r) = a\mu_0 w(r)/P_0$ or $\bar{w}(r) = \mu_0 w(r)/aq_0$
differential displacement, $\bar{w}_d = a\mu_0[w(0) - w(a)]/P_0$ or $\bar{w}_d = \mu_0[w(0) - w(a)]/aq_0$
bending moment, $\bar{M}_r(r) = M_r(r)/q_0a^3$
contact pressure, $\bar{p}(r) = p(r)/q_0$.

### *Numerical scheme*

The convergence and numerical stability of the variational scheme have been investigated with respect to the number of terms, $N$, in equation (1) and the number of ring elements, $M$, used to discretize the plate–soil contact surface $S$. The convergence and stability characteristics of the numerical solution are found to be nearly identical to those observed previously[18] for the plate–homogeneous soil interaction problem. It is found that accurate and stable solutions for displacements, stress resultants and contact pressure are obtained when $N \geqslant 6$ and $M > 15$. All numerical solutions presented in this paper correspond to $N = 8$ and $M = 20$.

As mentioned earlier, the present constraint variational scheme is based on Lagrange multipliers instead of the penalty function formulation used previously.[18] It was found[18] that the numerical solution is subjected to ill-conditioning for very large values of the penalty number. In the present formulation the boundary conditions are imposed exactly through Lagrange multipliers $\lambda_1$ and $\lambda_2$ which appear as basic unknowns in the linear equation system. In view of this, no ill-conditioning is encountered during the numerical solution.

The accuracy of the numerical solution, especially that of contact stress, is also controlled by the degree of accuracy adopted in the numerical evaluation of the influence function $f_{zz}(r, H; s_1, s_2)$. It is noted from the solution given in the preceding section that $f_{zz}$ appears in terms of an infinite integral with a complicated integrand and has to be evaluated by using an appropriate numerical integration scheme. Therefore the establishment of $[F]$ in equation (7) involves a considerable computational effort. A study of the integrand of the integral in equation

(18) indicates that it decays very slowly with the Hankel transform parameter $\xi$. The slow decay of the integrand is a consequence of the fact that the displacement is computed at the same level as the loading plane and this behaviour of the integrand contributes to further increase in the computational effort required for accurate numerical evaluation of $f_{zz}$. It is found that equation (18) can be written as

$$f_{zz} = \int_0^\infty (I_n - I_h) J_0(\xi r) \mathrm{d}\xi + \int_0^\infty I_h J_0(\xi r) \mathrm{d}\xi \tag{44}$$

where $I_h$ is the integrand corresponding to a homogeneous half-space with shear modulus equal to $\mu(H)$. The second infinite integral in the above equation is explicitly given by Selvadurai and Rajapakse[21] and can be evaluated without using numerical integration. It is noted that the term $I_n - I_h$ in the first infinite integral of equation (44) decays much faster than $I_n$ along with increasing $\xi$ owing to similar asymptotic behaviour. This enables efficient and accurate numerical integration of the first integral. The above procedure has been used to compute $f_{zz}$ in all numerical solutions presented in this paper.

*Comparison with rigid anchor solution*[15]

Previous studies on footing/anchor response have been concerned mainly with homogeneous soils, except the studies by Rowe and Booker[15,16] where the elastic response of *rigid anchors/footings* in a non-homogeneous soil was considered. In view of this, only a limited comparison can be presented. Table I presents a comparison of the axial stiffness of a rigid plate anchor in a linearly non-homogeneous elastic soil. The solutions presented by Rowe and Booker[15] agree very closely with those obtained from the present analysis. The minor difference observed in Table I can be attributed to the fact that in Reference 15 the linearly non-homogeneous soil is modelled as a multilayered elastic medium whereas the present solutions are based on an exact analytical representation of the non-homogeneous soil.

*Response of surface footings*

Figure 2 shows the variation of dimensionless central deflection $\bar{w}(0)$ and differential deflection $\bar{w}_d$ of a uniformly loaded circular footing ($\nu_p = 0{\cdot}3$) with the footing rigidity parameter $K_r$ and the degree of soil non-homogeneity, $\bar{m}$. Note that $\bar{m} = 0$ represents a homogeneous soil medium. It is observed that footings with $K_r > 100$ exhibit characteristics of rigid footings and the degree of soil non-homogeneity, $\bar{m}$, has a significant influence on the settlement of the footing. The central

Table I. Comparison of solutions of a rigid plate anchor

| | $P_0/\mu(\bar{H})aw(0)$ | | | |
|---|---|---|---|---|
| | $\mu_0/\mu(\bar{H}) = 0{\cdot}5$ | | $\mu_0/\mu(\bar{H}) = 0{\cdot}05$ | |
| $\bar{H}$ | Present study | Rowe and Booker[15] | Present study | Rowe and Booker[15] |
| 2 | 15·7 | 16·0 | 17·7 | 17·7 |
| 4 | 15·3 | 15·9 | 16·3 | 16·7 |
| 6 | 15·2 | 15·8 | 15·9 | 16·4 |
| 8 | 15·2 | 15·8 | 15·7 | 16·4 |

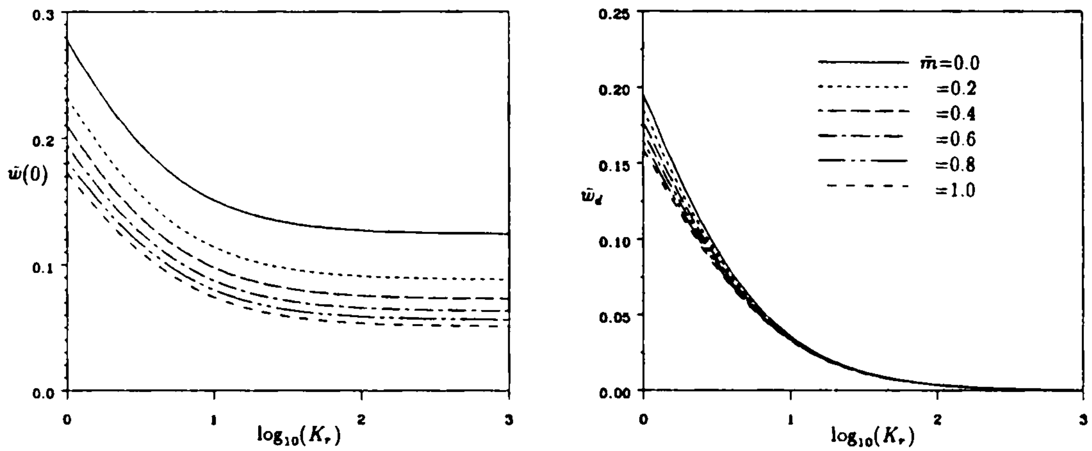


Figure 2. Variation of normalized (a) central deflection and (b) differential deflection of a uniformly loaded surface footing with relative rigidity $K_r$ and degree of non-homogeneity, $\bar{m}$

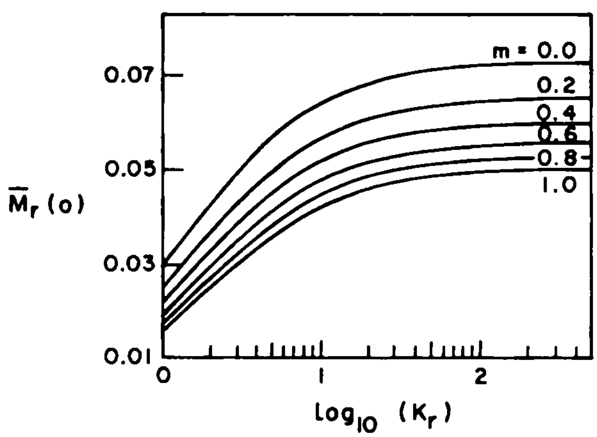


Figure 3. Variation of normalized central bending moment of a uniformly loaded surface footing with relative rigidity $K_r$ and degree of non-homogeneity, $\bar{m}$

deflection of the footing decreases rapidly with increasing $\bar{m}$ owing to the stiffening response of the supporting soil. For example, the central displacement of a footing resting on a non-homogeneous soil with $\bar{m} = 1$ is less than one-half that of an identical footing on a homogeneous soil. The central deflection also decreases gradually with increasing value of the footing rigidity $K_r$ and approaches a limiting value for $K_r > 100$. It is noted from Figure 2(b) that the differential deflection of a flexible footing ($K_r < 100$) decreases with increasing degree of non-homogeneity of the supporting soil, and as a consequence a sharp variation of $\bar{w}_d$ with $K_r$ is observed for homogeneous soils when compared to non-homogeneous soils.

Figure 3 shows the variation of central bending moment of a uniformly loaded footing with $K_r$ and $\bar{m}$. The general trend of variation of $\bar{M}_r(0)$ with $K_r$ is similar for all values of $\bar{m}$. However, the magnitude of $\bar{M}_r(0)$ decreases rapidly with increasing degree of soil non-homogeneity. This behaviour is consistent with the decreasing differential deflection with increasing $\bar{m}$ observed in Figure 2(b). Figures 4(a) and 4(b) show the variation of radial bending moment profiles of a uniformly loaded surface footing with the rigidity parameter $K_r$ and the degree of non-homogeneity, $\bar{m}$, respectively. The bending moment throughout the footing is found to increase with increasing values of $K_r$. This behaviour is observed for all values of $\bar{m}$. The solutions presented in Figure 4(b) indicate that the bending moments within the footing decrease with increasing degree of soil non-homogeneity. In addition, the percentage decrease of central bending moment of the footing when $\bar{m}$ is varied from 0 to 1 is found to be higher for flexible footings than for rigid footings.

Figures 5(a) and 5(b) show the variation of contact stress profile of a uniformly loaded footing with the rigidity $K_r$ and the degree of non-homogeneity, $\bar{m}$, respectively. It is found that for all values of $\bar{m}$ the contact stress within the region $0 < r/a < 0{\cdot}7$ decreases with increasing rigidity of the footing. This results in some redistribution of contact stress near the footing edge, and the classical singular behaviour of the contact stress as $r \rightarrow a$ is also observed. The contact stress profiles presented in Figure 5(b) show a slight increase in the magnitude of contact stress within the region $0 < r/a < 0{\cdot}7$ when the degree of soil non-homogeneity is varied from 0 to 1. This behaviour is noted for all values of the rigidity parameter $K_r$, and the percentage increase in contact pressure near the plate centre is found to be higher for rigid footings.

Figures 6(a) and 6(b) show the variation of central and differential deflection respectively of a centrally loaded surface footing with the rigidity $K_r$ and the degree of soil non-homogeneity, $\bar{m}$. The general variation of $\bar{w}(0)$ with $\bar{m}$ and $K_r$ is similar to that observed in Figure 2 for uniformly loaded footings. However, the percentage decrease in the central deflection is higher for centrally loaded footings when $K_r$ is varied from 1 to 500. Under loading of equal magnitude, flexible footings subjected to concentrated loads experience a higher differential deflection than uniformly loaded footings. Numerical solutions for bending moment and contact stress profiles of centrally loaded surface footings were also studied. The influence of $\bar{m}$ and $K_r$ on the solutions is found to be similar to that observed earlier for uniformly loaded footings. However, the bending moment profile shows a singularity at $r = 0$ and the contact pressure also shows a gradual increase in magnitude towards the footing centre with decreasing rigidity. In addition to the above numerical studies, the response of the footing was also examined for different values of Poisson's ratio $\nu_p$ of the footing. It is found that the footing displacements decrease by nearly 15% and the bending moments increase marginally when $\nu_p$ is varied from 0 to 0·5. The influence of $\nu_p$ is found to be negligible on contact stress profiles.

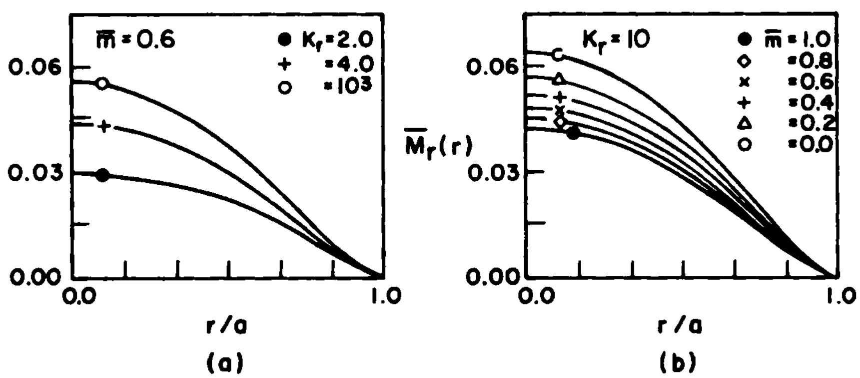


Figure 4. Variation of radial bending moment profiles of a uniformly loaded footing with (a) relative rigidity parameter $K_r$ and (b) degree of non-homogeneity, $\bar{m}$

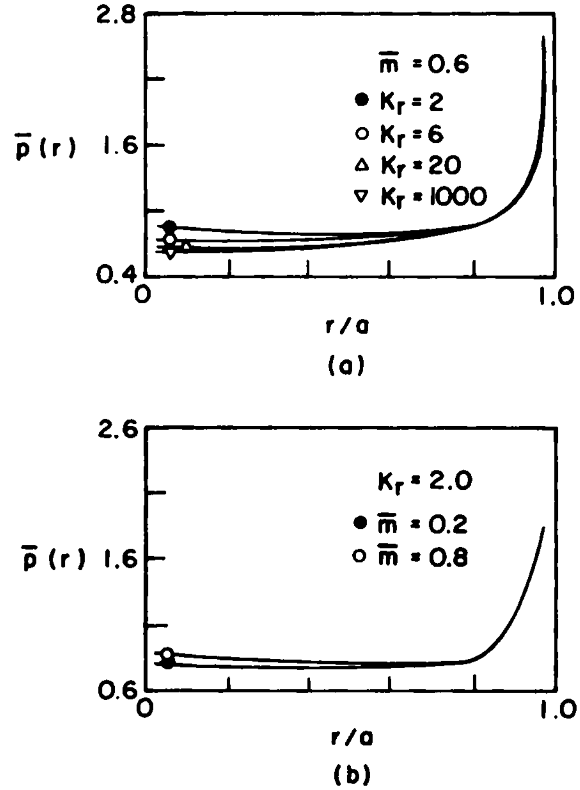


Figure 5. Variation of contact stress profiles of a uniformly loaded footing with (a) relative rigidity parameter $K_r$ and (b) degree of non-homogeneity, $\bar{m}$

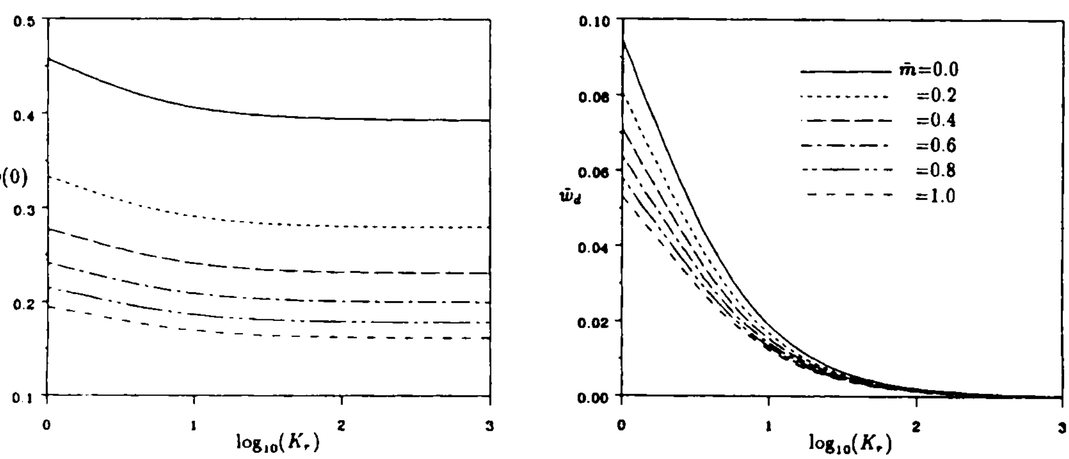


Figure 6. Variation of normalized (a) central deflection and (b) differential deflection of a centrally loaded surface footing with relative rigidity $K_r$ and degree of non-homogeneity, $\bar{m}$

*Response of anchor plates*

The displacements of flexible anchor plates in non-homogeneous soils are considered in this subsection. In the parametric study the degree of soil non-homogeneity, $\bar{m}$, is varied from 0 (homogeneous) to 1 and the anchor rigidity $K_r$ is varied from 1 to 1000. The depth of embedment of the anchor, $\bar{H}$, is assumed to vary between 0·5 and 10. Figures 7 and 8 show the variation of normalized central deflection $\bar{w}(0)$ and differential deflection $\bar{w}_d$ respectively of an anchor buried

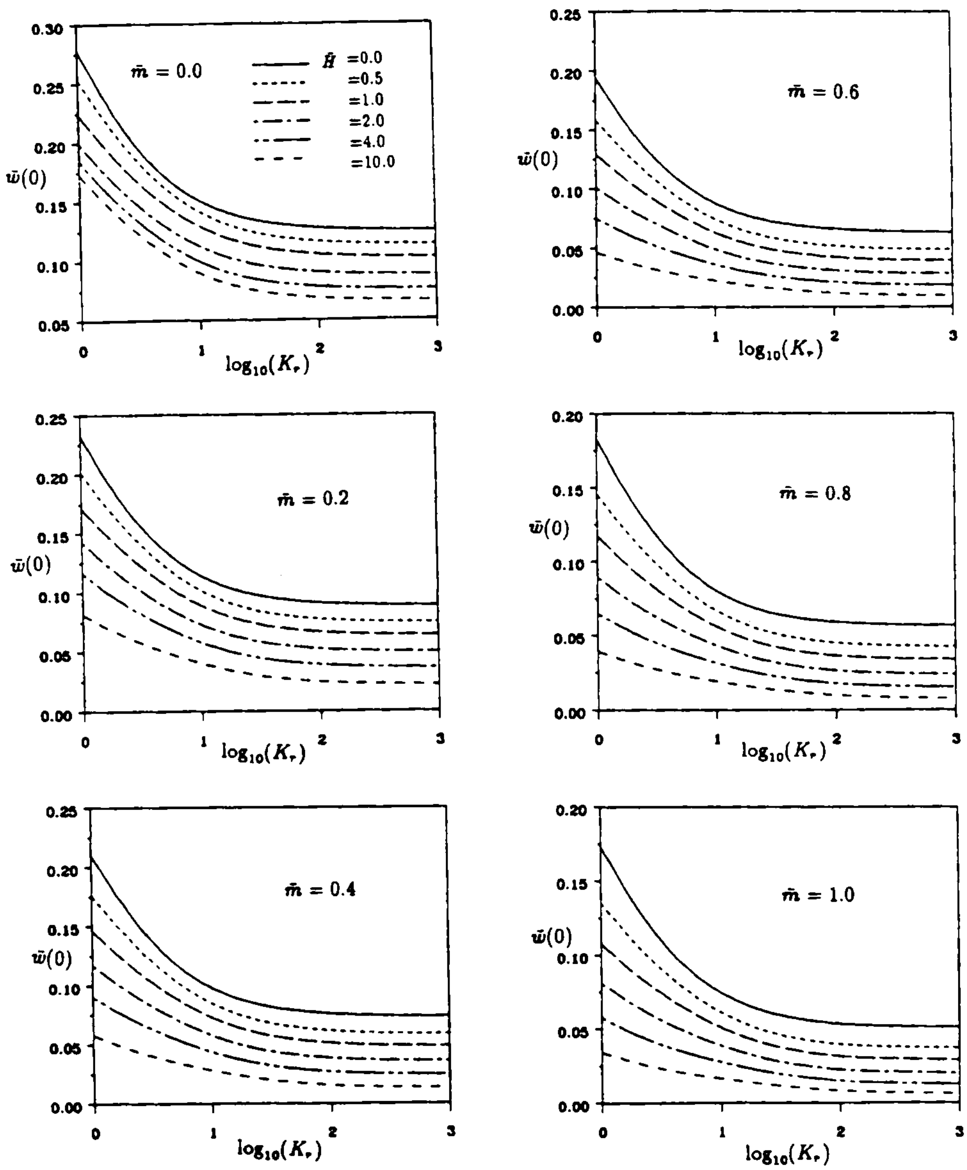


Figure 7. Variation of normalized central deflection of anchor plates with relative rigidity $K_r$ and degree of non-homogeneity, $\bar{m}$

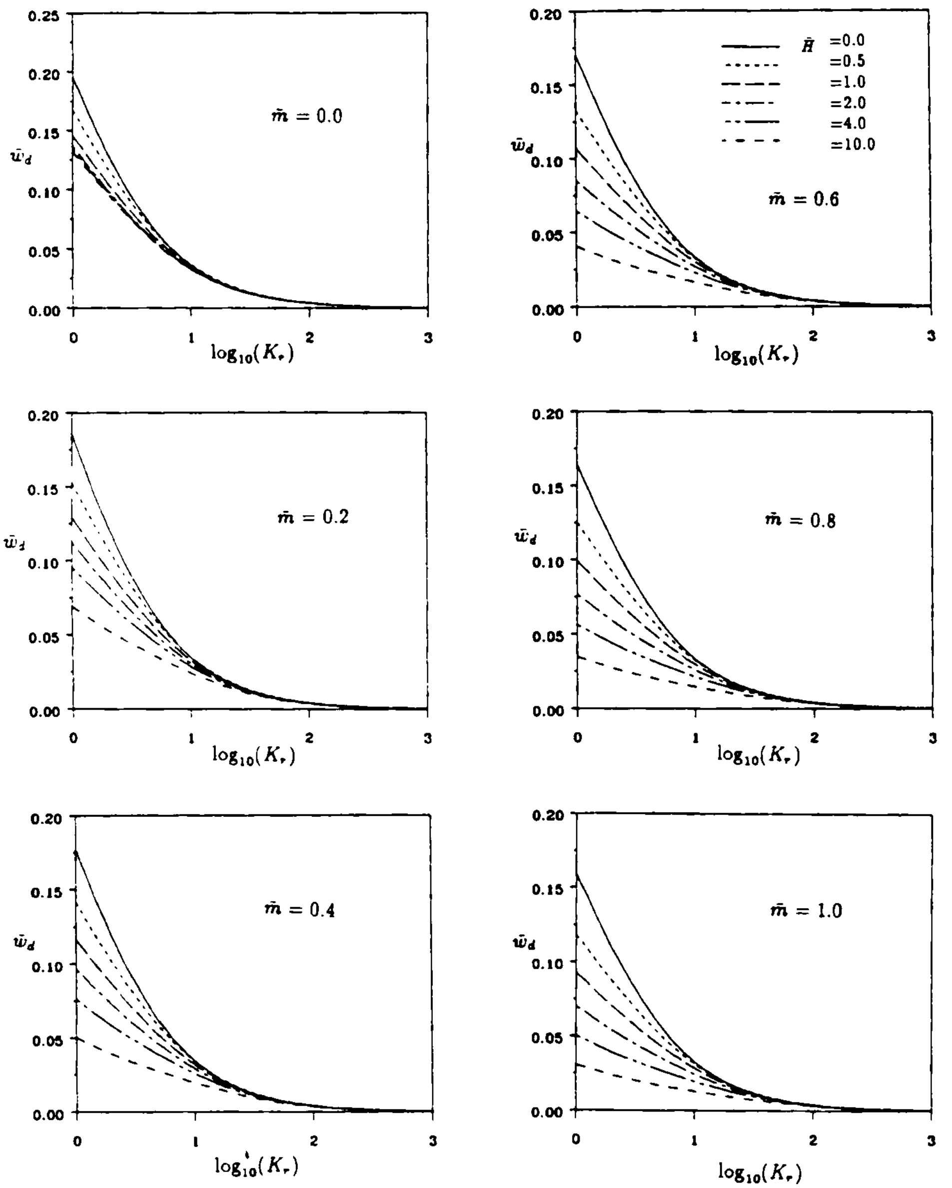


Figure 8. Variation of normalized differential deflection of anchor plates with relative rigidity $K_r$ and degree of non-homogeneity, $\bar{m}$

in a non-homogeneous soil. Comparison of numerical results indicates that both the central displacement and the differential deflection decrease with increasing depth of embedment of the anchor up to a depth $\bar{H} = 10$, while beyond this value the response is found to be independent of $\bar{H}$. In addition, anchors with $K_r > 100$ exhibit characteristics of rigid anchors irrespective of the values of $\bar{m}$ and $\bar{H}$. The numerical results presented in Figures 7 and 8 also indicate that the degree of soil non-homogeneity significantly influences the response of the anchor. The general trend is a

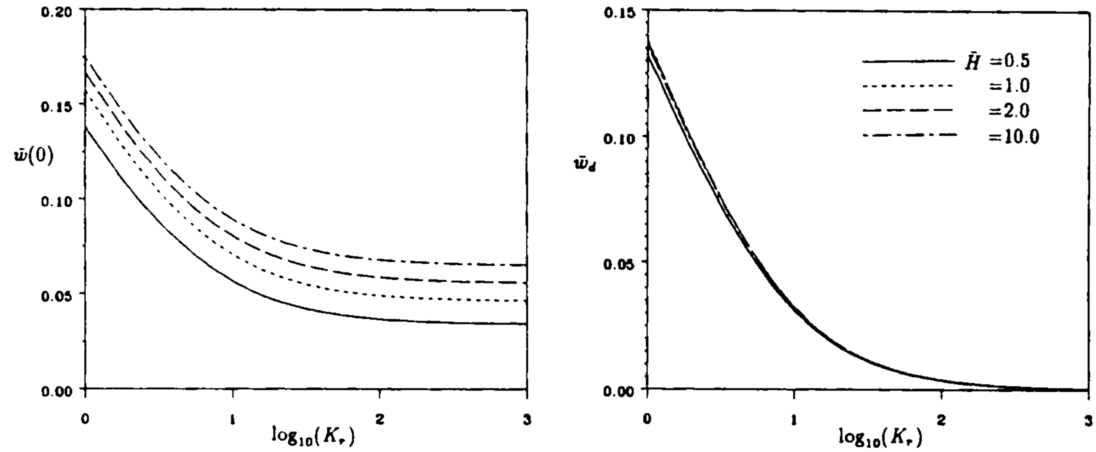


Figure 9. Variation of normalized (a) central deflection and (b) differential deflection of anchor plates with relative rigidity $K_r$ and depth of embedment, $\bar{H}$, for a soil with $\mu_0 = 0$

decrease in both the central displacement and the differential displacement with increasing $\bar{m}$ for an anchor located at a given depth. The differential deflections of deeply buried anchors in non-homogeneous soils are much smaller than the corresponding deflections for anchors in homogeneous soils. This is consistent with the fact that the soil becomes stiffer with depth as $\bar{m}$ is increased and results in more resistance for deformation of the anchor. The range of variation of central and differential displacements with the anchor flexibility is found to be smaller for anchors located deep below the surface when compared to near-surface anchors.

Figure 9 shows the variation of $\bar{w}(0)$ and $\bar{w}_d$ of an anchor plate in a non-homogeneous soil with a surface shear modulus equal to zero ($\mu_0 = 0$). The normalized displacements $\bar{w}(0)$ and $\bar{w}_d$ and the rigidity parameter $K_r$ are defined with respect to the shear modulus at the depth of the anchor. Note that for the soil profile under consideration the degree of non-homogeneity, $\bar{m}$, decreases with increasing $\bar{H}$. Therefore in Figure 9(a), $\bar{w}(0)$ is found to increase with the anchor depth up to $\bar{H} = 10$, while beyond this depth the response is found to be independent of $\bar{H}$. Figure 9(b) indicates that $\bar{w}_d$ is essentially independent of $\bar{H}$ for the present case. The general variation of $\bar{w}(0)$ and $\bar{w}_d$ with the rigidity parameter $K_r$ is similar to that observed previously for soils with $\mu_0 \neq 0$.

## CONCLUSIONS

The response of a flexible circular footing/anchor in a linearly non-homogeneous elastic soil is analyzed by using a variational method of analysis. The numerical stability and the convergence of the solution scheme have been verified. Numerical solutions indicate that the central deflections of both uniformly and centrally loaded footings decrease with increasing degree of non-homogeneity of the soil. Similar behaviour is also observed for differential deflection of the footing. In addition, the deflection of the footing decreases rapidly with increasing values of the relative rigidity parameter $K_r$ of the footing, and footings with $K_r > 100$ can be treated as rigid. The magnitude of the central bending moment of a uniformly loaded footing decreases rapidly with increasing degree of non-homogeneity of the soil and increases gradually with the relative rigidity for $K_r < 100$. Contact stress profiles of uniformly loaded footings show a decrease in magnitude near the central region with increasing $K_r$. The influence of the degree of non-homogeneity of the soil on the contact stress profile is found to be almost negligible. It is noted that both the central displacement and differential deflection of anchor plates decrease with increasing depth of embedment up to a value $\bar{H} = 10$, while beyond this value the response is essentially independent of the depth of embedment. Anchor plates with relative rigidity greater than 100 can be treated as rigid anchors irrespective of the values of $\bar{H}$ and $\bar{m}$. As in the case of surface footings, the displacements of the anchor also decrease with increasing degree of non-homogeneity of the soil. However, the degree of influence of soil non-homogeneity is more pronounced for anchor plates than for surface footings.

## ACKNOWLEDGEMENT

The work described in this paper was supported by grants A-6507 and A-3866 from the Natural Science and Engineering Research Council of Canada.

## REFERENCES

1. A. P. S. Selvadurai, *Elastic Analysis of Soil–Foundation Interaction, Developments in Geotechnical Engineering Vol. 17* Elsevier, Amsterdam, 1979.
2. A. W. Skempton and D. J. Henkel, 'Tests on London clay from deep boring at Paddington, Victoria and the South Bank', *Proc. Fourth Int. Conf. on Soil Mechanics, Vol. 1*, London 1957, pp. 100–106.
3. W. H. Ward, S. G. Samuels and M. E. Butler, 'Further studies of the properties of London clay', *Géotechnique*, **9**, 33–58 (1959).
4. W. H. Ward, A. Marsland and S. G. Samuels, 'Properties of the London clay at the Ashford Common Shaft', *Géotechnique*, **15**, 321–344 (1965).
5. J. B. Burland and J. A. Lord, 'The load–deformation behaviour of Middle Chalk at Mundford, Norfolk', *Proc. Conf. In situ Investigations in Soil and Rocks*, British Geotechnical Society, London, 1969, BRS Paper 6/70.
6. C. P. Abbiss, 'A comparison of the stiffness of the chalk at Mundford from a seismic survey and a large scale tank test', *Géotechnique*, **29**, 461–468 (1978).
7. R. E. Gibson, 'The analytical method in soil mechanics', *Géotechnique*, **24**, 115–140 (1974).
8. R. E. Gibson, 'Some results concerning displacements and stresses in a non-homogeneous elastic half space', *Géotechnique*, **17**, 58–67 (1967).
9. R. E. Gibson and G. C. Sills, 'On the loaded elastic half space with depth varying Poisson's ratio', *J. Appl. Math. Phys. (ZAMP)*, **20**, 691–695 (1969).
10. R. E. Gibson and G. C. Sills, 'Settlement of a strip load on a nonhomogeneous orthotropic imcompressible elastic half space', *Q. J. Mech. Appl. Math.*, **28**, 233–243 (1975).
11. R. E. Gibson, P. T. Brown and K. R. F. Andrews, 'Some results concerning displacement in a nonhomogeneous elastic layer', *J. Appl. Math. Phys. (ZAMP)*, **22**, 855–864 (1971).
12. A. O. Awojobi and R. E. Gibson, 'Plane strain and axially symmetric problems of a linearly nonhomogeneous elastic half space', *Q. J. Mech. Appl. Math.*, **26**, 285–302 (1973).
13. R. E. Gibson and G. S. Kalsi, 'The surface settlement of a linearly inhomogeneous cross-anisotropic elastic half space', *J. Appl. Math. Phys. (ZAMP)*, **25**, 843–847 (1974).
14. P. T. Brown and R. E. Gibson, 'Surface settlement of a deep elastic stratum whose modulus increases linearly with depth', *Can. Geotech. J.*, **9**, 467–473 (1972).
15. R. K. Rowe and J. R. Booker, 'The elastic displacements of single and multiple underream anchors in a Gibson soil', *Géotechnique*, **31**, 125–141 (1980).
16. R. K. Rowe and J. R. Booker, 'The behaviour of footings resting on a non-homogeneous soil mass with a crust, Part II—Circular footings', *Can. Geotech. J.*, **18**, 265–279 (1981).
17. A. P. S. Selvadurai, 'Elastic contact between a flexible circular elastic plate and a transversely isotropic elastic half space', *Int. J. Solids Struct.*, **16**, 167–176 (1980).
18. R. K. N. D. Rajapakse, 'The interaction between a circular elastic plate and a transversely isotropic elastic half-space', *Int. J. Numer. Anal. Methods Geomech.*, **12**, 419–436 (1988).
19. S. P. Timoshenko and S. Woinowsky-Krieger, *Theory of Plates and Shells*, 2nd edn, McGraw-Hill, New York, 1959.
20. K. Washizu, *Variational Methods in Elasticity and Plasticity*, 3rd, edn, Pergamon, New York, 1982.
21. A. P. S. Selvadurai and R. K. N. D. Rajapakse, 'On the load transfer from rigid cylindrical inclusion into an elastic half space', *Int. J. Solids Struct.*, **21**, 1213–1229 (1985).
22. R. K. N. D. Rajapakse, 'Rigid inclusion in nonhomogeneous incompressible elastic half space', *J. Eng. Mech., ASCE*, **116**, 399–410 (1990).
23. M. Abramowitz and I. A. Segun, *Handbook of Mathematical Functions*, 5th edn, Dover, New York, 1968.
24. I. N. Sneddon, *Fourier Transforms*, McGraw-Hill, New York, 1951.